NONLINEAR CHROMATICITY CORRECTION FOR THE INTERACTION REGION OF SUPER TAU-CHARM FACILITY

Linhao Zhang†, Ye Zou, Tao Liu, Jingyu Tang
School of Nuclear Science and Technology, University of Science and Technology of China, Hefei, Anhui, China

Abstract

The Super Tau-Charm Facility is a new-generation electron-positron collider in the beam energy range of 1-3.5 GeV, with a target luminosity exceeding 5×10^{34} cm^{-2}s^{-1} at 2 GeV using a large Piwinski angle and crab-waist collision scheme. However, the required sub-millimeter vertical beta function ($\beta_y^* < 1$ mm) induce strong nonlinear chromaticity, which severely limits the momentum aperture of the collider rings and leads to a very short Touschek lifetime. To achieve the necessary 1.5% momentum aperture, local correction of the nonlinear chromaticity from the final-focus quadrupoles is essential. In this paper, we derive the theoretical origin of the nonlinear chromaticity and demonstrate dedicated measures to systematically mitigate these nonlinearities order by order. Specifically, we present an updated modular linear lattice for the interaction region to facilitate nonlinear chromaticity optimization. The second-order dispersion at the crab sextupoles is also reduced to nearly zero. By implementing a local chromaticity correction scheme up to the third order, we obtain a momentum aperture of 2% for the interaction region.

INTRODUCTION

The Super Tau-Charm Facility (STCF), proposed in China, is a new-generation high-luminosity electron-positron collider operating in the low-energy range of 1-3.5 GeV [1]. To achieve the target luminosity exceeding 5×10^{34} cm^{-2}s^{-1}, a collision scheme combining a large Piwinski angle and crab-waist correction is adopted. However, the required high beam current, low emittance, and an extremely low vertical beta function ($\beta_y^* < 1$ mm) lead to a very short Touschek lifetime. In particular, the strong nonlinear chromaticity induced by the sub-millimeter β_y^* constitutes a major limitation on the momentum aperture of the collider rings. To improve the Touschek lifetime, a momentum aperture of 1.5% is essential.

A dedicated design of the crab-waist interaction region (IR) for the STCF has been presented [2] and integrated into the collider rings [3], yielding a momentum apperture of approximately ±1.5% and a Touschek lifetime exceeding 300 s at the luminosity of 0.94×10^{35} cm^{-2}s^{-1} and beam energy of 2 GeV. However, residual vertical second-order and horizontal third-order chromaticity originating in the IR, as well as the leakage of second-order dispersion from the IR into the arcs, remain the main factors limiting the momentum aperture. In this paper, we first analyze the chromaticity in a single-pass transport line and identify local correction measures for the IR nonlinear chromaticity. We then update the IR optics design to improve the nonlinear chromaticity correction and reduce the leakage of second-order dispersion from the IR.

CHROMATICITY IN A SINGLE-PASS TRANSPORT LINE

In a single-pass transport line (e. g., one half of the IR), chromaticity is defined as the rate of change of the particle betatron oscillation phase advance with respect to the relative momentum deviation δ. The dependence of the focusing gradient of all magnetic elements on δ is the fundamental cause of chromatic effects. Following Anton's derivation of high-order chromaticity for a ring [4], when considering an off-momentum particle with momentum deviation δ in a transport line, the first- to third-order derivatives of the betatron phase advance μ_z can be expressed as:

$$\frac{\mathrm{d}\mu_z(\mathrm{s})}{\mathrm{d}\delta} = \mp\frac{1}{2}\int_0^s \beta_z(K_1 - K_2D_0)\,\mathrm{d}s' - \frac{a_{1,z}(s)}{2}, \quad (1)$$

$$\frac{\mathrm{d}^2\mu_z(\mathrm{s})}{\mathrm{d}\delta^2} = -2\frac{\mathrm{d}\mu_z(\mathrm{s})}{\mathrm{d}\delta} + \int_0^s \frac{b_{1,z}^2 - a_{1,z}^2}{\beta_z}\mathrm{d}s' \pm \int_0^s \beta_z\left(K_2D_1 + K_3\frac{D_0^2}{2}\right)\mathrm{d}s' \mp \int_0^s \beta_z b_{1,z}(K_1 - K_2D_0)\,\mathrm{d}s' - \frac{a_{2,z}(s)}{2}, \quad (2)$$

$$\frac{\mathrm{d}^3\mu_z(\mathrm{s})}{\mathrm{d}\delta^3} = 6\frac{\mathrm{d}\mu_z(\mathrm{s})}{\mathrm{d}\delta} + \int_0^s\left(-\frac{3a_{1,z}a_{2,z}}{\beta_z} + \frac{3a_{1,z}^2b_{1,z}}{\beta_z} - \frac{3b_{1,z}^3}{\beta_z} + \frac{3b_{1,z}b_{2,z}}{\beta_z}\right)\mathrm{d}s' \mp 3\int_0^s \beta_z\left[-\frac{K_4D_0^3}{6} + K_3\left(\frac{D_0^2}{2} - D_0D_1\right) + K_2(D_1 - D_2)\right]\mathrm{d}s' \mp \frac{3}{2}\int_0^s \beta_z b_{2,z}(K_1 - K_2D_0)\,\mathrm{d}s' - \frac{a_{3,z}(s)}{2}, \quad (3)$$

where z denotes the horizontal or vertical (i.e., x or y) plane, D_0, D_1, D_2 are the first-, second-, third-order dispersion functions respectively (satisfying $D_x(\delta)=D_0+D_1\delta+D_2\delta^2$), and $a_{n,z}$ and $b_{n,z}$ are chromatic Montague functions [5] extended to high order, defined as:

$$b_{n,z} = \frac{1}{\beta_z}\frac{\mathrm{d}^n\beta_z}{\mathrm{d}\delta^n}\Big|_{\delta=0}, a_{n,z} = \left(\frac{\mathrm{d}^n\alpha_z}{\mathrm{d}\delta^n} - \frac{\alpha_z}{\beta_z}\frac{\mathrm{d}^n\beta_z}{\mathrm{d}\delta^n}\right)\Big|_{\delta=0}. \quad (4)$$

Note that apart from the additional term of $-a_{n,z}/2$ appearing in Eqs. (1)-(3) for the single-pass system, all other terms are exactly equivalent to the high-order chromaticity expressions of a ring under periodic boundary conditions. In particular, Eq. (1) has also been given in Ref. [6].

Equations. (1-3) clearly indicates how different orders of chromaticity are generated and how they can be controlled and mitigated:

† zhanglinhao@ustc.edu.cn

- First-order chromaticity originates from the quadrupole gradient deviation experienced by particles with different momenta. It can be corrected by sextupoles placed at dispersive locations.
- Second-order chromaticity is mainly driven by the first order chromatic beta wave (i.e., first-order beta-beating) at quadrupoles. It is further affected by the second-order dispersion function and the first-order beta-beating at the sextupoles after implementing first-order chromaticity correction. Second-order chromaticity can be controlled by adopting octupoles at dispersive locations and by adjusting the phase advance between quadrupoles and chromaticity-correcting sextupoles (via tuning the $\beta_z b_{1,z}$ term).
- Third-order chromaticity mainly arises from the second-order beta-beating at quadrupoles. With first-order chromaticity correction implemented, the third-order chromaticity is additionally influenced by the first-order and second-order dispersion function at the chromaticity-correcting sextupoles. Decapoles placed at dispersive locations and sextupoles placed where the $\beta_z b_{2,z}$ term is large can be used to mitigate third-order chromaticity.
- Furthermore, we can easily infer from Eq. (3) that octupoles and decapoles located where $\beta_z b_{2,z}$ is large can be used to reduce fourth- and fifth-order chromaticity, respectively. Indeed, these are measures adopted in the FCC-ee IR lattice designed by P. Raimoni [7].

APPLICATION TO STCF IR

STCF IR Layout and Linear Optics

The STCF IR lattice adopts a modular optics design, as illustrated in Fig. 1. A half-IR of the STCF consists of the following modules: the final focus telescope (FFT), vertical chromatic correction (CCY), horizontal chromatic correction (CCX), crab sextupole section (CS), and multiple matching sections (MCY, YMX, XMC, and MS). The design proactively minimizes nonlinearities by implementing three core principles: (1) achieving exact -I transformations between chromatic sextupole pairs for geometric aberration cancellation; (2) minimizing the dispersion invariant H_x along the IR to enhance the local momentum aperture (LMA); and (3) optimizing the beta functions at the CS locations to reduce their strength and associated nonlinearities.

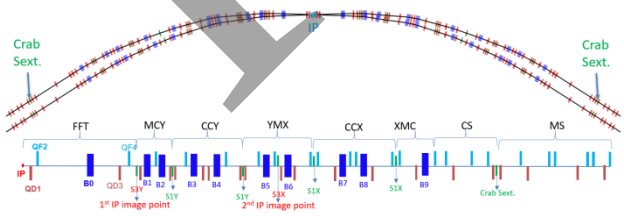

Figure 1: (Top) Layout of the complete IR for both rings; (bottom) detailed half-IR layout starting from IP.

The resulting optical functions, with $\beta_y^* = 0.8$ mm and $\beta_x^* = 40$ mm, for the STCF IR are shown in Fig. 2. A notable point is the maintenance of a low dispersion invariant H_x (≤ 0.025 m) throughout the IR, which enhances the LMA by reducing the nonlinear momentum dependence of particle trajectories. All dipoles have the same length of 1 m length for cost efficiency while preserving the required 1.5-2 m separation between the two rings. The total bending angle across the IR is 60°, consistent with the collider ring's geometric layout. To accommodate the 60 mrad IP crossing angle, an asymmetric 30 mrad split is applied: the outer-ring half-IR bends 30 mrad more, and the inner-ring half-IR 30 mrad less, resulting in an asymmetric dispersion distribution with respect to the IR.

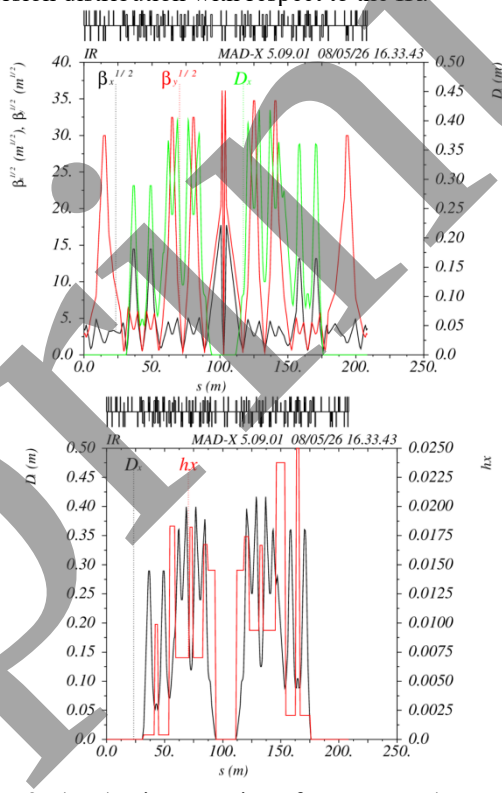

Figure 2: (Top) Linear optics of STCF IR; (Bottom) the corresponding dispersion and dispersion invariant.

Update on Local Chromaticity Correction

To obtain the desired Touschek lifetime for STCF, the target momentum aperture must be expanded to at least [-1.5%, +1.5%]. This necessitates order-by-order chromaticity compensation up to at least the third order for the STCF IR. Following the theoretical guidance presented above, the correction methodology is implemented as follows:

- First-order IR vertical and horizontal chromaticity is corrected by the main sextupole pairs with a -I map, S1Y and S1X (see Fig. 1), respectively;
- Second-order chromaticity is corrected by fine-tuning phase advances between S1Y/S1X and the IP;
- Third-order chromaticity in vertical and horizontal directions is corrected by additional sextupoles, S3Y and S3X, located at the 1st and 2nd image points of the IP, respectively.

However, the previous IR design shows a similar trend between the full-ring tune shift and the IR-only phase-advance variation with momentum deviation, see Fig. 3, which suggests that the momentum acceptance is primarily limited by residual vertical second-order and horizontal third-order chromaticity originating in the IR.

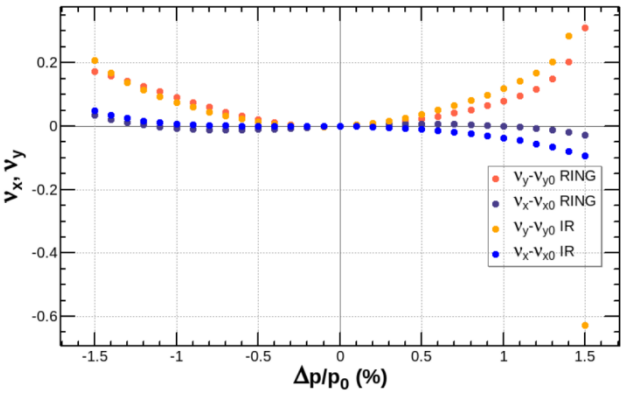

Figure 3: The tune variation with the momentum deviation for the ring and the phase advance variation for IR only.

Therefore, we reoptimize the IR optics by further tuning the phase advances from S1Y and S1X to the IP to reduce the second-order chromaticity, and by reoptimizing the strength of additional sextupoles, S3Y and S3X, at the IP image points to correct third-order chromaticity. Referring to the FCC-ee IR design [7], the variations of β and α at the IP versus momentum deviation are chosen as observables to evaluate the chromaticity correction performance of a half-IR (starting from the CS and ending at the IP). Furthermore, to mitigate adverse effects of crab sextupoles on the momentum aperture, the IR optics should exhibit minimal chromatic dependence at the CS locations. Thus, the chromatic amplitude function (W-function) and second-order dispersion should be close to zero at the CS locations.

The chromatic performance for the two half-IRs (i.e., IRLEFT and IRRIGHT) after reoptimization is shown in Figs. 4 and 5, respectively. From the variations of α at the IP versus δ, one can see that the first-order, second-order and third-order chromaticities have been well controlled within the momentum acceptance of [-2%, +2%]. Fourth-order and fifth-order chromaticities begin to dominate after the lower-order chromaticities have been corrected. In addition, the W function at the CS locations is well controlled, and the second-order dispersion is reduced to nearly zero, although its slope remains relatively large. This slope needs to be further optimized when the IR is matched to the arc sections.

It should be also mentioned that the required strength of additional sextupoles (S3X) is quite large (almost six times that of the main sextupole S1X). This is because the second-order beta beating at the S3X location is not sufficiently large. This issue demands further optimization of the IR linear optics in the future.

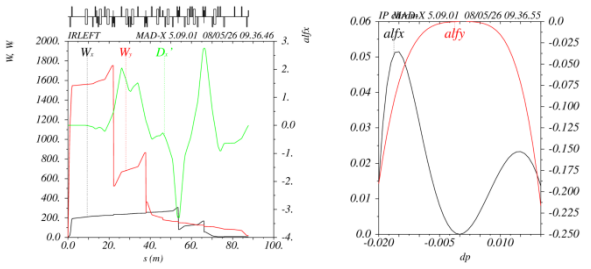

Figure 4: Chromatic performance for IRLEFT.

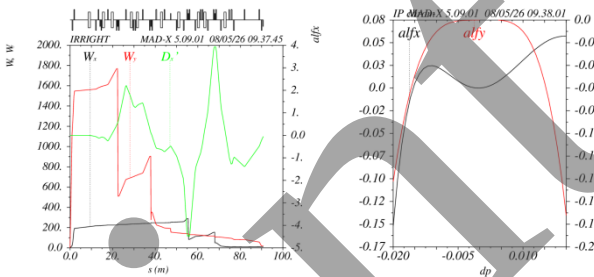

Figure 5: Chromatic performance for IRRIGHT.

CONCLUSION

This paper presents the theoretical formula for nonlinear chromaticity in a single-pass transport line, providing direct guidance for high-order chromaticity correction of a half-IR. Following this theory, we update the STCF IR optics, achieving well-mitigated first- to third-order chromaticities and well-controlled second-order dispersion. As a result, the momentum aperture is improved to 2%, exceeding the 1.5% requirement for the desired Touschek lifetime. Future work will focus on reducing the strength of additional sextupoles at the IP image points and matching the IR to the non-IR optics.

ACKNOWLEDGEMENTS

We thank P. Raimondi, A. Bogomyagkov, and D. Zhou for beneficial discussions. This work is jointly supported by National Natural Science Foundation of China (No. 12405174, No. 12341501), and Hefei Comprehensive National Science Center.

REFERENCES

[1] X.C. Ai, *et al.*, "Conceptual design report of the Super Tau-Charm Facility: the accelerator", *Nucl. Sci. Tech.*, vol. 36, p. 242, 2025. doi:10.1007/s41365-025-01833-x

[2] L.H. Zhang *et al.*, "Crab-waist interaction region design and integration for the Super Tau-Charm Facility", arXiv:2510.09198v2, 2025. doi:10.48550/arXiv.2510.09198

[3] Y. Zou *et al.*, "Optics design of the Super Tau-Charm Facility collider rings," *Nucl. Inst. Methods Phys. Res., Sect. A,* vol. 1084, no. 171191, Apr. 2026. doi:10.1016/j.nima.2025.171191

[4] A. Bogomyagkov, "Chromaticity correction of the interaction region", IAS Program on High Energy Physics, Hong Kong,18-21 January, 2016. http://ias.ust.hk/program/shared_doc/2016/201601hep/20160118_Bogomyagkov_LT.pdf

[5] B. W. Montague, "Linear optics for improved chromaticity correction", CERN-LEP-Note-165, 1979. https://cds.cern.ch/record/443342/

[6] Yunhai Cai *et al.*, "Optimization of chromatic optics in the electron storage ring of the Electron-Ion Collider", *Phys. Rev. Accel. Beams*, vol. 25, p. 071001, 2022. doi:10.1103/PhysRevAccelBeams.25.071001

[7] P. Raimondi *et al.*, "Local chromatic correction optics for Future Circular Collider e^+e^-", *Phys. Rev. Accel. Beams*, vol. 28, p. 021002, 2025. doi:10.1103/PhysRevAccelBeams.28.021002